Spin-polarized Inelastic Electron Tunneling Spectroscopy of Molecular Magnetic Tunnel Junctions

Wenyong Wang and Curt A. Richter

Semiconductor Electronics Division, National Institute of Standards and Technology, 100 Bureau Drive, M.S. 8120, Gaithersburg, Maryland 20899-8120, USA

Abstract. In this study, we fabricate molecular magnetic tunnel junctions and demonstrate that inelastic electron tunneling spectroscopy technique can be utilized to inspect such junctions to investigate the existence of desired molecular species in the device area. Tunneling magnetoresistance measurements have been carried out and spin-dependent tunneling transport has been observed. Bias-dependence of the tunneling resistance has also been detected. IETS measurements at different magnetic field suggested that the TMR bias-dependence was likely caused by the inelastic scattering due to the molecular vibrations.

Keywords: spin dependent transport, molecular self-assembly,
PACS: 72.25.–b; 81.16.Dn

INTRODUCTION

As recent research works have pointed out, molecular electronic devices with spin-dependent tunneling (SDT) transport behavior offer an innovative and extremely enticing direction towards spin electronics, both from fundamental and technological points of view. However, as for the case of traditional inorganic SDT devices, a strong bias-dependence of the junction magnetoresistance (JMR) has been observed in molecular spintronic devices, which may limit their practical applications. The physical mechanism of this dependence is unclear. In this work, inelastic electron tunneling spectroscopy (IETS) provides the unambiguous experimental evidence of the existence of molecular species in the molecular magnetic tunnel devices. We also use tunneling spectroscopy to investigate the spin-polarized inelastic electron tunneling processes in the molecular device for the first time, and show that inelastic scattering due to molecular vibrations, instead of magnon excitations, may be the main cause of the JMR bias-dependence. Tremendous progress has been made in the electronic transport characterizations of self-assembled monolayers (SAMs) in the past years [1, 2], especially with the application of the inelastic electron tunneling spectroscopy (IETS) technique that has been shown to be crucial in the identification of the molecular species confined inside a device area [3-6]. For example, tunneling transport has been determined as the main conduction mechanism for alkanethiol [CH3(CH2)n-1SH] SAMs formed on gold surfaces via such investigations [7, 8]. Recently, octanethiol [CH3(CH2)7SH] SAM, a member of the alkanethiol SAM family, has been used between two ferromagnetic electrodes to create an organic spintronic system [9], leading to the expectation that single molecules could be used as the ultimate building blocks for spintronic devices [10, 11]. However, although it is widely accepted that alkanethiols can form robust SAMs on gold surfaces [12], the SAM formation on ferromagnetic metals or metal oxide surfaces is still under investigation. In addition, even for the case of SAMs on gold, reliable controls and methods are required to validate true molecular transport in nanometer scale device structures [8]. Therefore, examinations are needed to verify that self-assembled molecules are indeed active components in these molecular magnetic tunnel junctions (MTJs). Furthermore, a strong bias-dependence of the junction tunneling magnetoresistance has been observed in the previous experiment, but the origin of this dependence is unclear in the published report [9]. This bias-dependence may limit practical application of molecular spintronic devices; therefore it is crucial to investigate the underlying physical mechanism. JMR bias-dependence is common in conventional metal-insulator-metal (M-I-M) MTJs [13, 14], and IETS

measurements at different magnetic fields have been attempted to study the magnon excitations in these devices to comprehend this phenomenon [15, 16]. In this study, we demonstrate that the IETS technique can be utilized to inspect MTJ junctions to confirm the existence of molecular species. We also apply the spin-polarized IETS technique, for the first time, to investigate inelastic scattering such as impurity-assisted tunneling processes [17, 18] in the molecular spintronic devices and show that the inelastic scattering due to molecular vibrations, instead of magnon excitations, may be the origin of the strong JMR bias-dependence in our samples. Our experimental results further support the theoretical argument that the spin-flip scattering interaction is weak in the molecular devices and therefore they could be useful structures for spin manipulations.

RESULTS AND DISCUSSIONS

Dc transport measurements and IETS characterizations of self-assembled molecules are performed by using the nanopore device that has been reported previously [7, 9, 19]. Unlike earlier IETS tunnel junctions [3], the nanopore devices use only the self-assembled molecules themselves as the tunnel barrier; thus oxide-free junctions are realized and intrinsic molecular properties can be investigated. Figure 1A schematically shows the nanopore device structure and the octanethiol molecule that forms the molecular tunnel barrier. Nanopore-based molecular-MTJs are fabricated as follows [9]: 150 nm Ni is thermally evaporated onto the topside of the sample to fill the pore and form one of the ferromagnetic electrodes. The device is then immediately transferred into a 5 mM solution of octanethiol with ethanol as the solvent for 24 h for SAM deposition [7, 9, 20]. The device is then rinsed and transferred to an evaporator, where 150 nm Co is thermally deposited under the pressure of 10^{-7} Torr onto the opposing side to encapsulate the SAM and form a completed device. During the second thermal evaporation step, liquid nitrogen is flowed through the sample holder to reduce thermal damage to the molecular layer as previously reported [7]. The device is subsequently packaged and loaded into a cryostat for electrical characterizations between 300 and 4.2 K. Inelastic electron tunneling spectra are obtained via direct lock-in second harmonic measurements [4]. Typical current-voltage [I(V)] characteristics of a MTJ with octanethiol molecules as the device component from room temperature to 4.2 K are presented in Fig. 1B. Positive bias corresponds to electrons injected from the bottom Co contact (Fig. 1A) through the molecular barrier to the top Ni contact. The Ni-octanethiol-Co devices in this study generally exhibit a minor thermally activated transport behavior unlike the alkanethiol SAM devices fabricated with gold electrodes, where a pure tunneling conduction has been observed [7]. For example, the device in Fig. 1B shows mild temperature-dependent conduction from room temperature to 50 K. Figure 1C is the corresponding Arrhenius plot, and a linear fitting on the data at 0.1 V and T > 50 K gives a thermal barrier of ~ 14 meV. The exhibition of this thermal activation indicates the existence of minor defects in the SAM [8]. Recent Fourier Transform Infrared (FTIR) measurements of a similarly formed (although large area) octanethiol SAM on a Ni surface suggest disordered monolayer formation [21], supporting the presence of defects in these thiol SAMs on Ni. At temperatures below 50 K, conduction is via pure tunneling as illustrated by the lack of temperature dependence shown in Fig. 1B. A current density of ≈ 1.3 x 10^4 A/cm2 is calculated at 0.5 V and T = 4.2 K by assuming a junction area of 50 nm in diameter, which is in agreement with previously reported results [8].

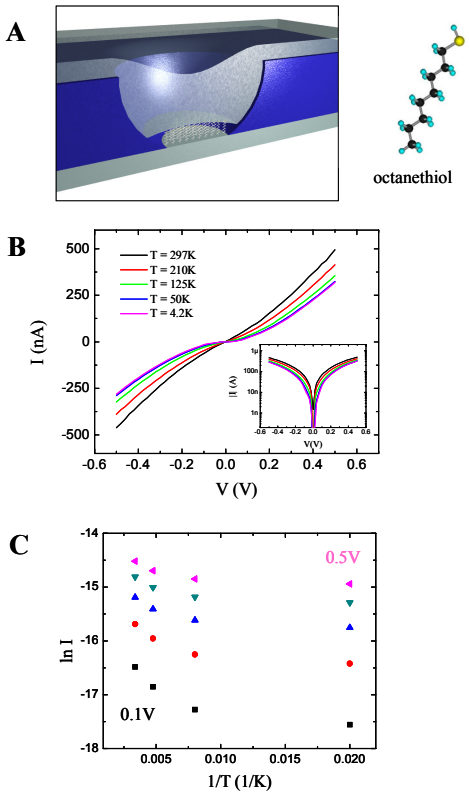

FIGURE 1. Device structure and temperature-dependent current-voltage [I(V)] characterizations. (A) Schematics of the nanopore device and chemical structure of the octanethiol molecule. The diameter of the nanopore is about 50 nm. (B) I(V) characteristics of the octanethiol MTJ device at selected temperatures of 297, 215, 125, 50 and 4.2 K. Inset shows the same data on a logarithmic scale. (C), Arrhenius plot generated from the I(V) data in (B) at selected voltages from 297 to 50 K. The voltage step is 0.1 V.

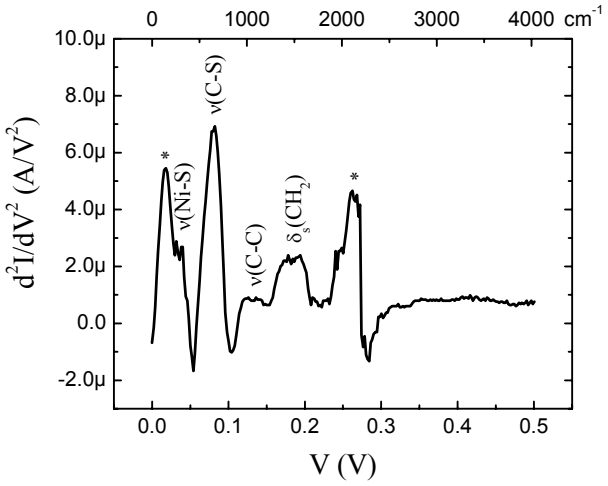

FIGURE 2. Inelastic electron tunneling spectrum of the molecular magnetic tunnel junction. The spectrum was obtained via lock-in second harmonic measurements with an ac modulation of 9.8 mV (RMS value) at a frequency of 503 Hz (T = 4.2 K). Molecular vibrational features from ν(Ni-S), ν(C-S), ν(C-C), and δ_s(CH2) modes are identified in the spectrum. Peaks labeled * are possibly due to a Ni phonon and the encasing Si3N4 membrane, respectively.

Figure 2 shows the inelastic electron tunneling spectrum of the same octanethiol MTJ device obtained at T = 4.2 K before applying the magnetic field, where the magnetizations of the two ferromagnetic electrodes are likely in a random configuration. An ac modulation of 9.8 mV (RMS value) at a frequency of 503 Hz was applied to the sample to acquire the second harmonic signals. Measurements at different dc resolutions and ac modulations were also performed to confirm the validity of the observed IETS spectra. The peaks at 81, 139, and 176 mV are assigned to ν(C-S), ν(C-C), and δ_s(CH2) modes of a surface-bound alkanethiolate from comparison with previously reported IETS, infrared (IR), Raman, and High Resolution Electron Energy Loss (HREEL) data [4, 22]. The shoulder appearing at ~ 40 mV is assigned to the ν(Ni-S) mode according to published experimental and theoretical studies [23, 24]. This ν(Ni-S) peak became more pronounced after the application of the external magnetic field. The peak at 262 mV is associated with the Si-H vibration related to the silicon nitride membrane that confines the SAM [4, 25]. The peak at 17 mV is possibly due to the contribution from nickel phonons [26]. The spectra of octanethiol SAM with ferromagnetic electrodes is quite different from the spectra of the octanedithiol SAM with gold as the electrodes, where almost all of the alkanethiol vibrational modes have been observed and a good agreement between experimental results and theoretical predictions on the peak intensities has been attained [4]. This difference could be caused by different molecule-metal contacts as well as the disordered monolayer formation inside the junction, as revealed by the thermally activated transport behavior from temperature-dependent I(V) measurements. As theoretical calculations have pointed out, IETS spectra are very sensitive to the intermolecular conformation and molecular-metal contact geometry changes [27-29]. Besides, the dithiol molecule used in the previous experiment could form two chemisorbed contacts with the gold electrodes and realize an upright SAM geometry that gives near-perfect dipole moment configurations, which produced proper peak intensity preferences [4]. Nonetheless, the obtained tunneling spectra in this study exhibited vibrational signatures of the molecules, thus confirming the presence of the molecular species confined inside the Ni-octanethiol-Co magnetic tunnel junctions.

Tunneling magnetoresistance measurements were carried out to investigate the spin-dependent transport in these molecular junctions. Figure 3A is the plot of the change of the junction resistances ($R = \frac{V}{I}$) [9] of the same device as a function of magnetic field at a dc bias of 10 mV at T = 4.2 K. The field was applied out of the sample plane. Catastrophic damage to the molecular devices at high magnetic fields and high biases has been encountered; therefore, in order to save the device for spin-polarized IETS measurements the applied field for JMR measurements was restricted to |H| < 0.6 T and the bias was < 50 mV. When the magnetic field applied to the device was swept from positive to negative polarity, the junction resistance initially increased and showed a maximum at low magnetic fields. It then decreased at larger negative fields until the resistance became independent of the applied field at a value comparable to that observed at the initial high positive field (Fig. 3A). Based on these observations, we argue that an antiparallel configuration has been achieved at the low magnetic field where the junction showed the maximum resistance and a parallel configuration has been achieved at the negative field polarity where the

junction resistance became independent of the applied field. But under the conservative magnetic field conditions the resistance hysteresis loop did not close at the positive field side as shown in Fig. 3A. Asymmetric JMR behavior, similar to that in Fig. 3A, has been observed previously in similar molecular-MTJs, where a higher magnetic field was needed for one polarity to realize a parallel magnetization configuration [9]. The origin of this asymmetry in nanopore-based molecular-MTJs is unclear. Such asymmetric magnetoresistance phenomenon in traditional M-I-M MTJs has been reported before, where the asymmetry was caused by the exchange-biasing induced by antiferromagnetic layers in the sample structures [30-32]. In nanopore-based molecular-MTJs this asymmetry is possibly related to the specific device geometry that makes the magnetization of either electrode along one direction easier than the opposite direction. Such effects of the device geometry on magnetization processes in nanostructures have been discussed recently [33, 34]. It is difficult to fully understand the detailed configuration of the magnetization of the Ni and Co electrodes in the complex geometry of the nanopores, and we expect that the asymmetry is due in part to the fact that the applied magnetic field may not have been sufficient to fully saturate the metals [35]. Nevertheless, we presume that the loop in Fig. 3A would fully close and a parallel configuration would be achieved when the applied magnetic field is larger than +0.6 T in agreement with previously published data [9]. Thus, we attribute the observed magnetoresistance to spin-dependent transport through the molecular barrier.

Figure 3B shows the junction magnetoresistance at different dc biases. JMR was calculated according to the definition [9]: $JMR \equiv \frac{R_{\max} - R_P}{R_P}$, where R_{max} is the maximum resistance measured at low magnetic fields and RP is the resistance at the parallel magnetization configuration, which is defined as the resistance that shows field independence at the negative field polarity. As Fig. 3B shows, the device JMR has strong bias dependence, especially at voltages higher than 40 mV. Such JMR bias-dependence has been observed in most traditional M-I-M MTJs [13, 30], and it has been reported recently in molecular-MTJs as well [9]. Mechanisms of spin-flip scattering by magnon excitations at the ferromagnet/insulator interface [13, 36], impurity-assisted tunneling due to localized states inside the tunneling barrier [17, 18, 37], and ferromagnet density of states (DOS) changes as a function of applied bias [13] have been proposed to explain this bias-dependence. However, a consensus as to which of these mechanisms is the fundamental cause has yet to be reached.

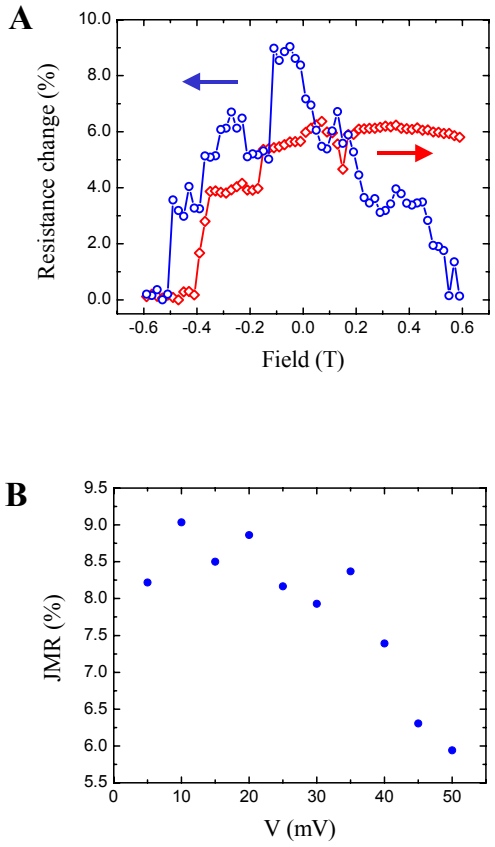

FIGURE 3. Tunneling magnetoresistance of the molecular junction. (A) Junction resistance change as a function of magnetic field at a dc bias of 10 mV and T = 4.2 K. The data were recorded when the applied magnetic field was swept from +0.6 to -0.6 T (circles) and then back to +0.6 T (diamonds). The arrows denote the field sweeping directions. (B) Device JMR as a function of bias at 4.2 K. A sharp decrease of JMR happened around 40 mV.

In this research, we utilized the spin-polarized IETS technique to investigate the JMR bias-dependence of the molecular-MTJs. Figure 4 shows the IETS spectra of the octanethiol MTJ device at different external magnetic fields. These spectra are characterized by four dominant peaks that were reproducibly observed at magnetic fields of -0.25, -0.5, and -0.75 T. The peaks at 42, 80, and 176 mV arise from molecular vibrations and are assigned as the molecule's ν(Ni-S), ν(C-S), and δ_s(CH2) vibrational modes, respectively. The peak at 270 mV is from the silicon nitride membrane that forms the device structure.

The initial application of an external magnetic field modifies the IETS spectrum. The small shoulder at 40 mV [due to ν(Ni-S)] became a distinct peak at a slightly higher position after the magnetic field was applied, while the peaks at 17 mV (due to Ni phonon) and 139 mV [due to ν(C-C)] became less dominant features. All of the spectra, whether taken before or after the introduction of the magnetic field, were obtained under the same test conditions and were stable and repeatable upon successive measurements. Hence the observed variations were not caused by random instrumentation errors. The changes in the IETS spectrum are possibly related to changes of the molecule-metal contact geometry, or the electronic structures (e.g., the DOS) of the ferromagnetic electrodes, or both, which could be introduced upon the application of the magnetic field. Further theoretical and experimental investigations are needed to fully comprehend this issue.

After the two ferromagnetic electrodes have been magnetized, the IETS spectra (Fig. 4) remain essentially the same at biases larger than 50 mV as the device was changed from the antiparallel (low magnetic fields) to the parallel (high negative magnetic fields) magnetization configurations. Magnon excitations in conventional M-I-M MTJs have previously been investigated by inelastic tunneling spectroscopy studies at different magnetization configurations of the ferromagnetic electrodes [15, 16, 38]. Typically only a magnon feature is observed in these experiments, and no significant spectral changes except that caused by the magnon excitations are reported between parallel and antiparallel configurations [16, 38], which is in agreement with our data. In our study reported here, no magnon excitation was observed in the spin-polarized IETS spectra (Fig. 4), which suggests that the JMR bias-dependence shown in Fig. 3B was not caused by spin-flip scattering processes in the molecular junction. However, well-defined peaks due to electron-molecule couplings have been detected, and the first peak position at 42 mV corresponds very well to the onset of the rapid JMR decrease at about 40 mV shown in Fig. 3B; therefore, the JMR bias-dependence in this molecular-MTJ device was attributed to the inelastic scattering due to the molecular vibrations. The inelastic scatterings from intrinsic molecular vibrations or nonmagnetic impurities are spin-independent processes and contribute conductance increases for both parallel and antiparallel magnetization configurations, which decrease the junction tunneling magnetoresistance [13].

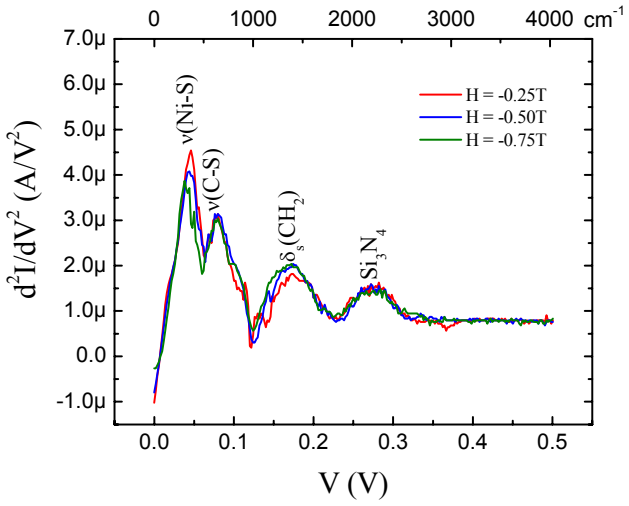

FIGURE 4. Spin-polarized IETS characterizations of the octanethiol magnetic tunnel junction. The spectra are obtained at 4.2 K at magnetic fields of -0.25, -0.5, and -0.75 T. Four pronounced peaks appear, and the first peak position corresponds well to the onset of the abrupt decrease of the JMR at 40 mV shown in Fig. 3B.

CONCLUSION

In this study, IETS characterizations of the molecular magnetic tunnel junction unambiguously confirmed the presence of molecular components in the tunnel junction. This verification is critical, for it clearly illustrates that molecules form the tunnel barrier in these MTJ devices and clarifies the physical picture of the device configuration by excluding other possible spin-dependent transport processes such as tunneling through nickel oxide or titanium oxide from the previous experiment [9]. Combined with further theoretical investigations, the obtained data will be able to provide vital information for a better understanding of the SAM formation on the surfaces of ferromagnets in nanometer scale device structures. The spin-polarized IETS technique is used here for the first time to inspect inelastic tunneling processes in molecular-MTJs, and the results revealed that the decrease of device JMR is correlated with the onset of the excitation of molecular vibrations. This observation supports previous arguments that the spin-flip scattering and spin-orbital interaction are weak in the molecular-MTJ devices and therefore they could be useful structures for spin manipulations [9-11]. However, this examination also illustrates that inelastic scattering events due to the molecular vibrational excitations must be accounted for when predicting the performance of practical molecular spintronic devices. Finally, this study demonstrates that the spin-polarized IETS technique can be used to investigate multiple physical processes (i.e., magnon

and phonon excitations) in a broad range of different device structures (i.e., organic and inorganic). As an example, in a recent theoretical study the spin-polarized IETS technique has been proposed to directly measure the spin excitation spectrum of a spin array that has potentially important applications for a wide range such as quantum computing and data storage [39].

ACKNOWLEDGMENTS

We thank D. DeLongchamp, D. Gundlach, C. Hacker, O. Kirillov, M. Stiles, J. Suehle, and E. Vogel for helpful discussions. This work was supported in part by the DARPA MoleApps Program. The fabrication was performed at the NIST Advanced Measurement Laboratory Nanofab and the Cornell Nano-Scale Science & Technology Facility..

REFERENCES

1. A. Aviram, M. A. Ratner, Eds., Molecular Electronics: Science and Technology (The Annals of the New York Academy of Sciences, Vol. 852, New York, 1998).
2. G. Cuniberti, G. Fagas, K. Richter, Eds., Introducing Molecular Electronics (Lecture Notes in Physics, Vol. 680, Springer, Berlin, 2005).
3. P. K. Hansma, Ed., Tunneling Spectroscopy: Capabilities, Applications, and New Techniques (Plenum, New York, 1982).
4. W. Wang, T. Lee, I. Kretzschmar, M. A. Reed, Nano Lett. 4, 643 (2005).
5. J. G. Kushmerick et al., Nano Lett. 4, 639 (2004).
6. M. A. Reed, Nature Materials 3, 286 (2004).
7. W. Wang, T. Lee, M. A. Reed, Phys. Rev. B 68, 035416 (2003).
8. W. Wang, T. Lee, M. A. Reed, Rep. Prog. Phys. 68, 523 (2005).
9. J. R. Petta, S. K. Slater, D. C. Ralph, Phys. Rev. Lett. 13, 136601 (2004).
10. E. G. Emberly, G. Kirczenow, Chem. Phys. 281, 311 (2002).
11. A. R. Rocha et al., Nature Materials 4, 335 (2005).
12. A. Ulman, An Introduction to Ultrathin Organic Films from Langmuir-Blodgett to Self-Assembly (Academic Press, Boston, 1991).
13. E. Y. Tsymbal, O. Mryasov, P. R. LeClair, J. Phys.: Condens. Matter 15, R109 (2003).
14. I. Zutic, J. Fabian, S. Das Sarma, Rev. Mod. Phys. 76, 323 (2004).
15. J. S. Moodera, J. Nowak, R. J. M. van de Veerdonk, Phys. Rev. Lett. 80, 2941 (1998).
16. J. Murai et al., Jpn. J. Appl. Phys. 38, L1106 (1999).
17. A. M. Bratkovsky, Phys. Rev. B 56, 2344 (1997).
18. A. M. Bratkovsky, Appl. Phys. Lett. 72, 2334 (1998).
19. K. S. Ralls, R. A. Buhrman, R. C. Tiberio, Appl. Phys. Lett. 55, 2459 (1989).
20. Z. Mekhalif, F. Laffineur, N. Couturier, J. Delhalle, Langmuir 19, 637 (2003).
21. C. A. Hacker, unpublished result.
22. M. J. Hostetler, J. J. Stokes, R. W. Murray, Langmuir 12, 3604 (1996).
23. T. S. Rufael, D. R. Huntley, D. R. Mullins, J. L. Gland, J. Phys. Chem. 99, 11472 (1995).
24. H. Yang, T. C. Caves, J. L. Whitten, D. R. Huntley, J. Am. Chem. Soc. 116, 8200 (1994).
25. M. Molinary, H. Rinnert, M. Vergnat, P. Weisbecker, Mat. Sci. Eng. B 101, 186 (2003).
26. R. J. Birgeneau, J. Cordes, G. Dolling, A. D. B. Woods, Phys. Rev. B 30, A1359, (1964).
27. M. Galperin, A. Nitzan, M. A. Ratner, D. R. Stewart, J. Phys. Chem. B 109, 8519 (2005).
28. J. Jiang, M. Kula, W. Lu, Y. Luo, Nano Lett. 5 1551 (2005).
29. G. Solomon et al., J. Chem. Phys. 124, 094704 (2006).
30. J. S. Moodera, J. Nassar, G. Mathon, Annu. Rev. Mater. Sci. 29, 381 (1999).
31. M. Sato, K. Kobayashi, IEEE Trans. Mag. 33, 3553 (1997).
32. W. J. Gallagher et al., J. Appl. Phys. 81, 3741 (1997).
33. B. Tadic, K. Malarz, K. Kulakowski, Phys. Rev. Lett. 94, 137204 (1997).
34. C. C. Wang, A. O. Adeyeye, N. Singh, Nanotechnology 17, 1629 (2006).
35. It is possible that the observed magnetoresistance was due to a mechanical change of the device structure, which could be caused by the ferromagnetic electrodes domain walls changing under the applied field. However, we feel this is unlikely the case because in these fragile devices magnetically induced mechanical changes appear to cause catastrophic damage.
36. S. Zhang, P. M. Levy, A. Marley, S. S. P. Parkin, Phys. Rev. Lett. 79, 3744 (1997).
37. J. Zhang, R. White, J. Appl. Phys. 83, 6512 (1998).
38. J. Schmalhorst, S. Kammerer, G. Reiss, A. Hutten, Appl. Phys. Lett. 86, 052501 (2005).
39. S. Salahuddin, S. Datta, Phys. Rev. B 73, 081301(R) (2006).